The effect of simvastatin on chemotactic capability of SDF-1α and the promotion of bone regeneration

Yun-Song Liu [a,1], Meng-En Ou [b,1], Hao Liu [c], Ming Gu [a], Long-Wei Lv [a], Cong Fan [a], Tong Chen [a], Xiang-Hui Zhao [a], Chan-Yuan Jin [a], Xiao Zhang [a], Yun Ding [b], Yong-Sheng Zhou [a,d,*]

[a] Department of Prosthodontics, Peking University School and Hospital of Stomatology, Beijing 100081, China
[b] The 3rd Dental Clinic, Peking University School and Hospital of Stomatology, Beijing 100081, China
[c] The Core Laboratory, Peking University School and Hospital of Stomatology, Beijing 100081, China
[d] National Engineering Lab for Digital and Material Technology of Stomatology, Peking University School and Hospital of Stomatology, Beijing 100081, China

ARTICLE INFO

ABSTRACT

The purpose of this study was to investigate the cooperative effects of simvastatin (SIM) and stromal cell-derived factor-1α (SDF-1α) on the osteogenic and migration capabilities of mesenchymal stem cells (MSCs), and construct a cell-free bone tissue engineering system comprising SIM, SDF-1α and scaffold. We found that 0.2 μM SIM significantly increased alkaline phosphatase activity ($P < 0.05$) of mouse bone marrow MSCs with no inhibition of cell proliferation, and enhanced the chemotactic capability of SDF-1α ($P < 0.05$). Next, we constructed a novel cell-free bone tissue engineering system using PLGA loaded with SIM and SDF-1α, and applied it in critical-sized calvarial defects in mice. New bone formation in the defect was evaluated by micro-CT, HE staining and immunohistochemistry. The results showed that PLGA loaded with SIM and SDF-1α promoted bone regeneration significantly more than controls. We investigated possible mechanisms, and showed that SDF-1α combined with SIM increased MSC migration and homing in vivo, promoted angiogenesis and enhanced the expression of BMP-2 in newly-formed bone tissue. In conclusion, SIM enhanced the chemotactic capability of SDF-1α and the cell-free bone tissue engineering system composed of SIM, SDF-1α and scaffold promoted bone regeneration in mouse critical-sized calvarial defects.

1. Introduction

Bone tissue engineering has been widely studied. Many investigators [1–5] have succeeded in regenerating bone defects with different kinds of seed cells, including bone marrow derived mesenchymal stem cells (BMMSCs) and adipose-derived stromal cells (ASCs). Cell delivery has been the classical approach in bone regeneration. But this strategy presents several notable shortcomings, such as the high cost and time-consuming nature of ex vivo cell culture, the limited number of seed cells that can actually contribute to bone formation, and possible contamination and biological behavior change of the cells during cell expansion and passage [6–9].

How can we avoid the limitations of cell delivery? A cell-homing approach for tooth regeneration [10] provides a clue, as every single body contains BMMSCs which can differentiate into osteogenic cells. The key is to find a way to chemoattract them and induce them to differentiate along the osteoblastic lineage in situ, in order to finally achieve bone regeneration.

Stromal cell-derived factor 1 (SDF-1), a member of the CXC family of chemokines, includes several isoforms: SDF-1α, -β, -γ, -δ, -ε and -φ, which vary in the number of amino acid extensions at the carboxyl (C) [11], SDF-1 plays many important roles through activation of a G protein-coupled trans-membrane receptor CXC chemokine receptor-4 (CXCR4) [12,13]. SDF-1 signaling is not only essential for embryonic organ development [14–16], but is also important for maintaining postnatal tissue homeostasis [17–19]. In addition, there is increasing data suggesting SDF-1 signaling is necessary for repair or regeneration of brain [20], heart [21], muscle

* Corresponding author. Department of Prosthodontics, Peking University School and Hospital of Stomatology, 22 Zhongguancun Nandajie, Haidian District, Beijing 100081, China. Tel.: +86 10 82195370; fax: +86 10 62173402.
E-mail addresses: kqzhouysh@hsc.pku.edu.cn, kqzhouysh@gmail.com (Y.-S. Zhou).
[1] These authors contributed equally.

[22], liver [23], kidney [24], skin [25], tooth [26] and bone [26–28], via the recruitment of circulating or residing CXCR4-expressing MSCs. There is much evidence to suggest that MSCs can be chemoattracted by the delivery of SDF-1.

Moreover, bone regeneration requires osteogenic factors in addition to the seed cells. It is well known that several members of the bone morphogenetic protein (BMP) family, including BMP-2, -4, -6, -7, and -9 [29–37], can induce MSCs to undergo osteogenic differentiation and therefore promote bone formation. However, the application of BMPs has some disadvantages, including complicated synthesis, ease of degradation and high cost [38–40]. Our previous studies have shown that simvastatin (SIM), an inhibitor of the competitive 3-hydroxy-3-methyl coenzyme A (HMG-CoA) reductase, improves the osteogenesis of ASCs [41]. Meanwhile there have been many other studies demonstrating the bone promoting effects of the local application of SIM with different carriers in various animal models [42–45]. For these reasons, we decided to use SIM as an osteogenic growth factor. Furthermore, SIM has recently been shown to mobilize MSCs migrating to bone defects [46] or areas of spinal cord injury [47]. We therefore hypothesized that if we combined SDF-1α with SIM, SIM might enhance the chemotactic capability of SDF-1α and promote bone regeneration.

The purpose of this study was therefore to investigate the cooperative effects of SIM and SDF-1α on the osteogenic and migration capabilities of mesenchymal stem cells, and to construct a cell-free bone tissue engineering system composed of SIM, SDF-1α and scaffold.

2. Materials and methods

2.1. Isolation and maintenance of mouse BMMSCs

All materials were purchased from Sigma–Aldrich (St. Louis, MO, USA) unless otherwise stated. This study was approved by the Ethics Committee of the Peking University Health Science Center, Beijing, China (PKUSSIRB-2013023).

Mice from the Institute of Cancer Research (ICR) were sacrificed at 6–8 weeks old by CO_2 asphyxiation and their femurs and tibiae were carefully cleaned of adherent soft tissue. The tip of each bone was removed with a rongeur, and the marrow was harvested by inserting a syringe needle (27-gage) into one end of the bone and flushing with Dulbecco's Modified Eagle's Medium (DMEM; Gibco) [48]. Cells were cultured in maintenance medium (Dulbecco's Modified Eagle Medium containing 10% fetal bovine serum, 100 U/mL penicillin G and 100 μg/mL streptomycin) at 37 °C in an incubator with an atmosphere comprising 95% air and 5% CO_2 with 100% relative humidity. All cell-based experiments were repeated at least three times.

2.2. Cell proliferation assay

In cell proliferation assays, cells were cultured in maintenance medium (control group) or maintenance medium with various concentrations of SIM and/or SDF-1α (PeproTech Inc., NJ, USA). Cell number was determined using the cell-counting kit-8 (CCK8) according to the manufacturer's instructions (Dojindo Laboratories, Kumamoto, Japan). Growth curves were drawn using the absorbance values (mean ± SD, $n = 4$).

2.3. Cell differentiation assay

Cells were seeded in 24-well plates at a density of $1 \times 10^4/cm^2$ in maintenance medium alone or with various concentrations of SIM and/or SDF-1α. After 14 days of culture, the osteogenic differentiation of the cells was evaluated by alkaline phosphatase (ALP) activity assays using an ALP kit according to the manufacturer's protocol.

2.4. Cell migration assay

The effect of SIM and/or SDF-1α on mouse BMMSC (mBMMSC) migration was evaluated using a transwell migration assay [20]. Briefly, 1×10^5 cells cultured for 14 days were loaded into the upper chamber of a 24-well transwell plate (Corning, pore size 5 μm) and 600 μL medium containing different concentrations of SIM was added to the lower chamber. Twenty-four hours later, the filter was gently removed and the cells from the upper surface of the membranes were removed with a cotton swab. Cells that migrated to the lower surface of the membrane were fixed with 4% paraformaldehyde and stained for 10 min with 0.5% crystal violet. The number of cells that had migrated into the lower chamber was counted in five randomly selected microscopic fields (200×) per filter by blind evaluations performed twice by two independent assessors.

2.5. Bone regeneration in vivo by scaffolds loaded with SDF-1α and SIM

2.5.1. Preparation of the drug-loaded poly(lactide-co-glycolide) (PLGA) scaffolds

In order to construct a cell-free bone tissue engineering compound containing SDF-1α and SIM, processing solutions for the scaffolds were prepared as shown in Table 1. Twenty-four pieces of 4-mm diameter, 2-mm high cylindrical PLGA scaffold (lactide/glycolide: 75/25; Shandong Institute of Medical Instruments, China) were prepared and then soaked in 40 μL of processing solution for 15 min before grafting [49].

2.6. Animal experiments

Thirty-two 4-week-old, ICR mice were used in animal experiments. The mice were divided into four groups: (1) PLGA scaffold only, (2) PLGA scaffold loaded with SIM, (3) PLGA scaffold loaded with SDF-1α, and (4) PLGA scaffold loaded with SIM and SDF-1α. All animals were anesthetized by i.p. administration of pentobarbital sodium (7 mg/kg). A 1.5-cm sagittal incision was made on the scalp, and the calvarium was exposed by blunt dissection. A 4-mm diameter critical-sized defect was created at the left side of the calvarium by means of a trephine bur (Hager Meisinger GmbH, Neuss, Germany) under low speed drilling and copious saline irrigation. The periosteum of the defect region was removed carefully avoiding damage to the dura mater and brain. Occasional bleeding was stopped and the defect region was washed. The drug-loaded scaffolds were implanted into the defects, and the incisions were closed with sutures. At 3, 5 and 7 days after implantation, the animals were injected three times around the scaffold with 30 μL of the drug solution originally loaded into the scaffold.

2.7. Sample harvesting for long-term in vivo experiments

To investigate the bone regeneration capability of each group, five mice in each group were sacrificed by CO_2 inhalation 6 weeks after implantation. The implants and calvaria were carefully removed and sample preparation was performed as described previously [41].

2.8. Micro-computed tomography (micro-CT) and image analysis

To show bone formation in situ, micro-CT scans were performed using a high resolution Inveon Micro-CT (Siemens, Munich, Germany). The following experimental settings were used: an X-ray voltage of 80 kVp, anode current of 500 μA and an exposure time of 1500 ms for each of the 360 rotational steps. The images were used to reconstruct tomograms with a Feldkamp algorithm, using a commercial software package (Cobra EXXIM, EXXIM Computing Corp., Livermore, CA). Quantification of micro-CT images was then performed. New bone volume in the defects was evaluated by quantifying pixels in these regions using Inveon Research Workplace (Siemens, Germany).

2.9. HE staining and immunohistochemistry

All specimens were decalcified for 7 days in 10% EDTA (pH 7.4). Following decalcification, the specimens were dehydrated and subsequently embedded in paraffin. Sections (5 μm thickness) were stained with hematoxylin and eosin (HE). Osteogenesis was evaluated by immunohistochemical (IHC) analysis for osteopontin (OPN) and osteocalcin (OCN). To explore the mechanism of bone formation, IHC staining for CD34 and BMP-2 was performed to analyze angiogenesis [50] and the function of SIM.

2.10. Sample harvesting for short-term in vivo experiments

To explore the mechanism of bone formation, three mice in each group were sacrificed by CO_2 inhalation 1 week after implantation. The implants were separated carefully from mouse calvaria and embedded in optimal cutting temperature compound (Tissue-Tek; Sakura Finetek, Torrance, CA) and frozen sections for immunofluorescence staining were prepared.

2.11. Chemotactic capability of SIM- and SDF-1α-loaded scaffold in vivo

Immunofluorescence staining of frozen sections with a series of antibodies was used to determine the types of recruited cells [49]. MSCs were identified as stage-specific embryonic antigen-4 (SSEA4)+/CD45− [49–51]. Antibody staining was visualized by immunofluorescence with FITC- and Texas Red-conjugated secondary antibodies (Cell Signaling Technology Inc, USA). Cell nuclei were stained with 4′,6-

Table 1
Processing solutions for scaffolds.

Groups	Concentration of the solution	Solvent
Blank control	–	PBS with 2% DMSO
SIM	0.2 μM	PBS with 2% DMSO
SDF-1α	200 ng/ml	PBS with 2% DMSO
SIM and SDF-1α	SIM: 0.2 μM; SDF-1α: 200 ng/ml	PBS with 2% DMSO

diamino-2-phenylindole (DAPI). Stained sections were visualized using a Leica microscope and imaged with a CCD camera (Retiga EXi; Qimaging, Surrey, BC, Canada). The number of SSEA4+/CD45− MSCs in each group was counted in five randomly selected merged microscopic images by blind evaluations performed twice by two independent assessors.

2.12. Statistical analysis

Data are expressed as the mean ± standard deviation and were analyzed using SPSS software. One-way analysis of variance followed by Fisher's least significant difference test was performed. For all tests, statistical significance was accepted at P-values lower than 0.05.

3. Results

3.1. The effect of SIM and SDF-1α on the proliferation and differentiation of mBMMSCs

The effects of SIM at different concentrations on the proliferation of mBMMSCs proliferation are shown as growth curves (Fig. 1). CCK-8 assays demonstrated that SIM at 0.5 μM slowed cell growth, and cell proliferation was markedly inhibited at SIM concentrations higher than 0.5 μM. SIM concentrations of less than or equal to 0.2 μM had a negligible adverse effect on cell proliferation compared with the control group.

ALP activity in all SIM groups was significantly increased compared with the control group. In comparison with lower SIM concentrations, 0.2 μM SIM stimulated significantly higher levels of ALP activity in mBMMSCs.

Next, we tested the effects of SDF-1α on the proliferation and differentiation of mBMMSCs and found that SDF-1α at concentrations of 50, 100, 200 and 400 ng/ml had no significant effects on cell proliferation and osteogenic differentiation.

3.2. The effect of SIM on chemotactic capability of SDF-1α in vitro

As has been reported in many studies, we found that SDF-1α had a positive effect on the migration capacity of mBMMSCs. At SDF-1α concentrations of 50, 100, 200 and 400 ng/ml the migration capacity of mBMMSCs was significantly increased compared with control groups (Fig. 2). There was no significant difference between the 200 and 400 ng/ml SDF-1α groups. Interestingly, we found that SIM at concentrations of 0.1 and 0.2 μM also significantly increased cell migration by 30.7% and 36.0%. More importantly, when combined with 0.2 μM SIM, the chemotactic capability of SDF-1α was further enhanced. The migration capacities of mBMMSCs cultured in 50 ng/ml SDF-1α + SIM, 100 ng/ml SDF-1α + SIM, 200 ng/ml SDF-1α + SIM and 400 ng/ml SDF-1α + SIM were significantly increased by 63.3%, 63.5%, 91.1% and 80.0% compared to the corresponding groups without SIM.

3.3. Cooperative effect of SIM and SDF-1α on bone regeneration in critical-sized calvarial defects

3.3.1. Radiological assessment of bone formation

To assess new bone formation in the bone defects, micro-CT was performed and the results are shown in Fig. 3A. In the control group, scanning revealed an almost complete lack of healing in empty defects. In the SIM group, small numbers of high density spots were observed. In the SDF-1α group, small peninsulas of bone nodule formation along the margins of the defect were observed. In the SIM + SDF-1α group, tissues with markedly greater bone density were observed in the defects. Quantification of micro-CT images (Fig. 3B) provided further evidence that significantly more
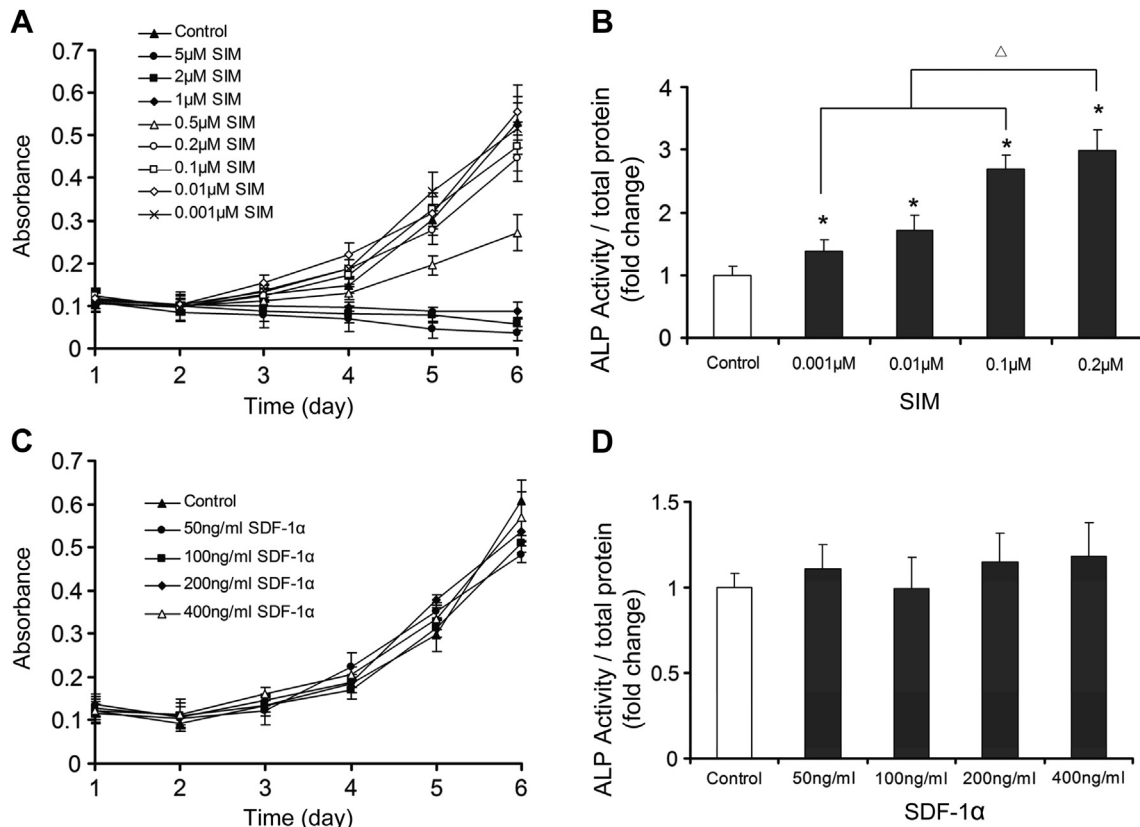
Fig. 1. The effect of SIM and SDF-1α on the proliferation and differentiation of mBMMSCs. (A) Growth curves, measured using a CCK-8 kit, and (B) ALP activity of mBMMSCs cultured in different concentrations of SIM. (C) Growth curves and (D) ALP activity of mBMMSCs cultured on different concentrations of SDF-1α. *$P < 0.05$ compared with control group; Δ$P < 0.05$ compared with other SIM groups.
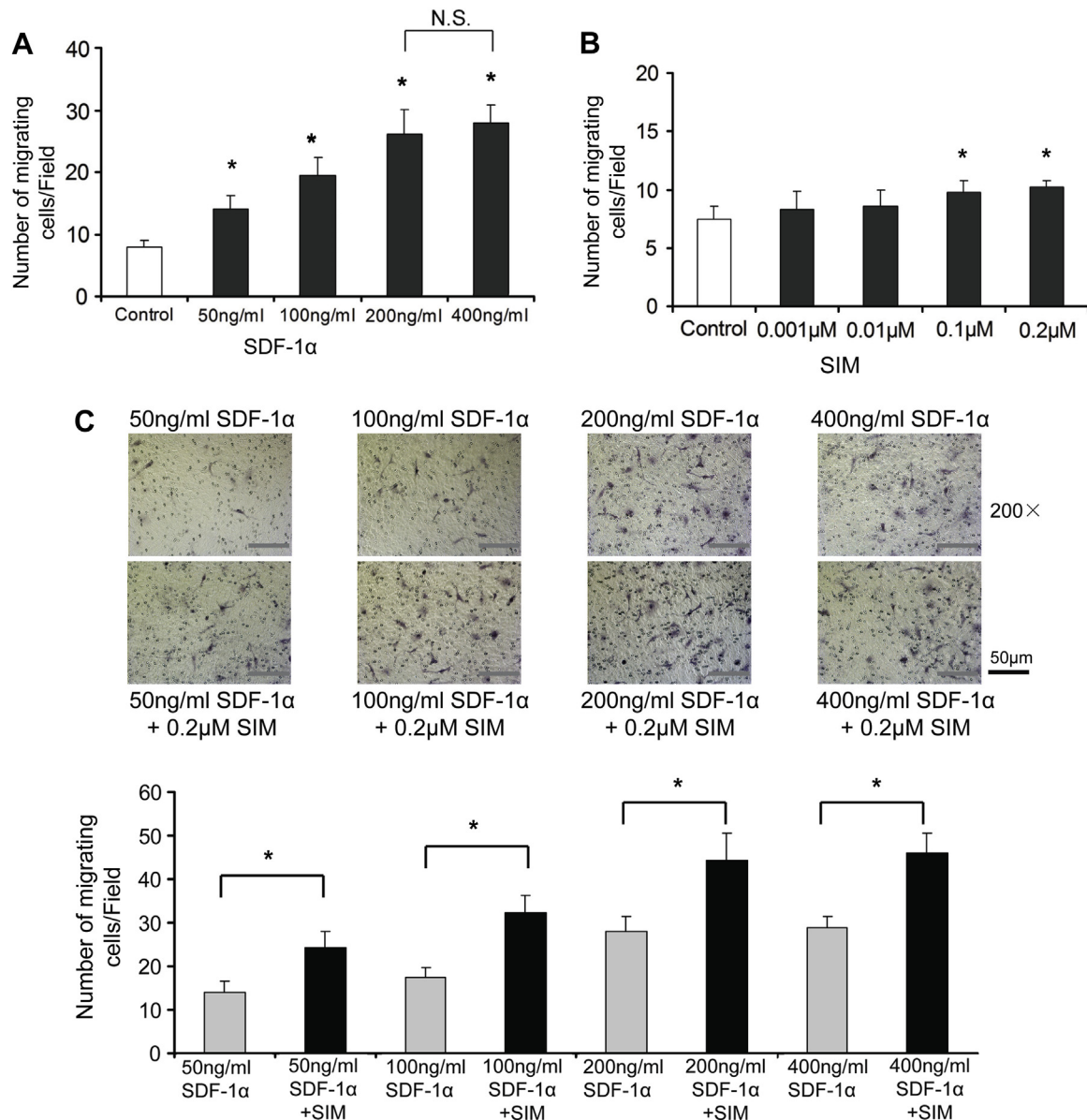
Fig. 2. The in vitro chemotactic capability of SDF-1α was enhanced when combined with SIM. (A) SDF-1α had positive effect on the migration capacity of mBMMSCs in transwell assays. (B) SIM at concentrations of 0.1 and 0.2 μM also increased cell migration. (C) The chemotactic capability of SDF-1α could be further significantly enhanced when combined with 0.2 μM SIM. *$P < 0.05$; N.S., not significant.

bone was formed in the SIM + SDF-1α group than in the other three groups ($P < 0.05$).

3.3.2. Histological assessment of bone formation

HE staining of representative sections from each group is shown in Fig. 4A. In the control and SIM groups, the defect area was occupied by connective tissue, and no typical bone tissue was observed. In the SDF-1α group, more bone-like tissues could be seen especially near the border of the bone defect. In the SIM + SDF-1α group, markedly greater amounts of bone-like tissue formed not only along the border but also in the center of the bone defect.

The results of IHC staining are shown in Fig. 4B. We found that the osteogenic markers OPN and OCN were highly expressed in both the SDF-1α group and the SIM + SDF-1α group. Moreover the SIM + SDF-1α group showed higher expression of OPN and OCN than the SDF-1α group.

3.4. Cooperative effect of SIM and SDF-1α on recruitment of MSCs in vivo

Immunofluorescence staining for SSEA-4 (green) and CD45 (red) in histological sections is shown in Fig. 5A. SSEA-4-positive and CD45-negative (SSEA-4+/CD45−) cells were considered to be MSCs [49–51]. The control group and the SIM group had very low engraftment of MSCs, whereas the SDF-1α group and the SIM + SDF-1α group had greater levels of MSC engraftment. Moreover, there was greater recruitment of MSCs in the SIM + SDF-1α group than in the any of the other three groups ($P < 0.05$).

3.5. Cooperative effect of SIM and SDF-1α on angiogenesis in vivo

IHC staining of tissue sections from the bone defect regions for CD34 showed that markedly more CD34-positive vascular
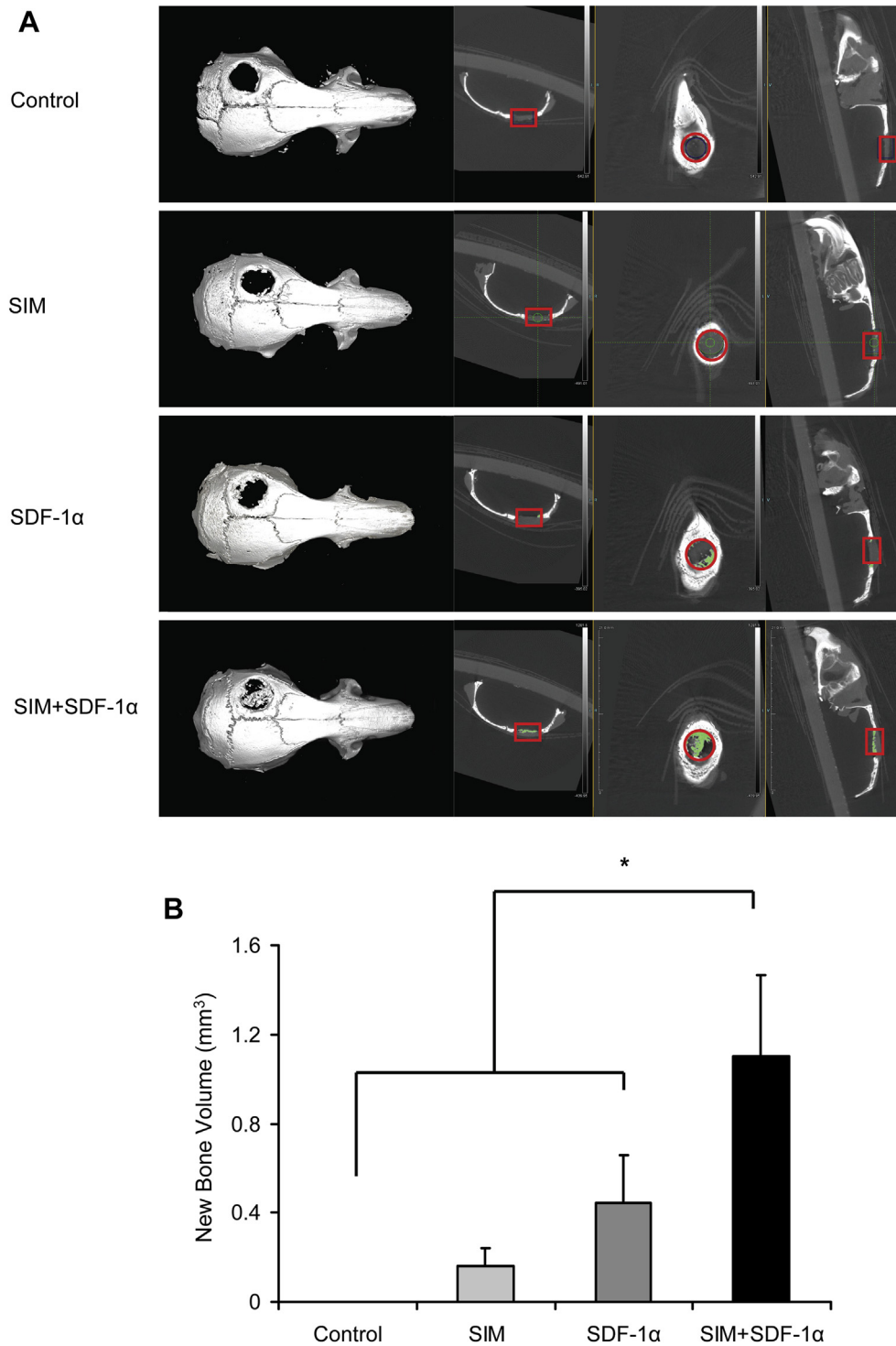
Fig. 3. SDF-1α combined with SIM increased bone formation in critical-sized calvarial defects in mice. Mice were treated with PLGA scaffolds alone (control) or loaded with SIM, SDF-1α or a combination of SIM + SDF-1α. (A) Micro-CT images of bone formation in each group after 6 weeks. (B) Quantitative comparison of new bone volume among the different groups. *$P < 0.05$.

endothelium cells were present in the SIM + SDF-1α group than in the other three groups (Fig. 6).

3.6. The effect of SIM on expression of BMP-2 in newly-formed bone tissue

IHC staining for BMP-2 in typical newly-formed bone tissue from the SDF-1α and the SIM + SDF-1α groups demonstrated a higher level of expression of BMP-2 in the SIM + SDF-1α group (Fig. 7). No typical new bone structure was observed in either the control or SIM groups.

4. Discussion

In order to investigate the potential for bone formation by cell homing without cell delivery, a tissue-engineered bone system
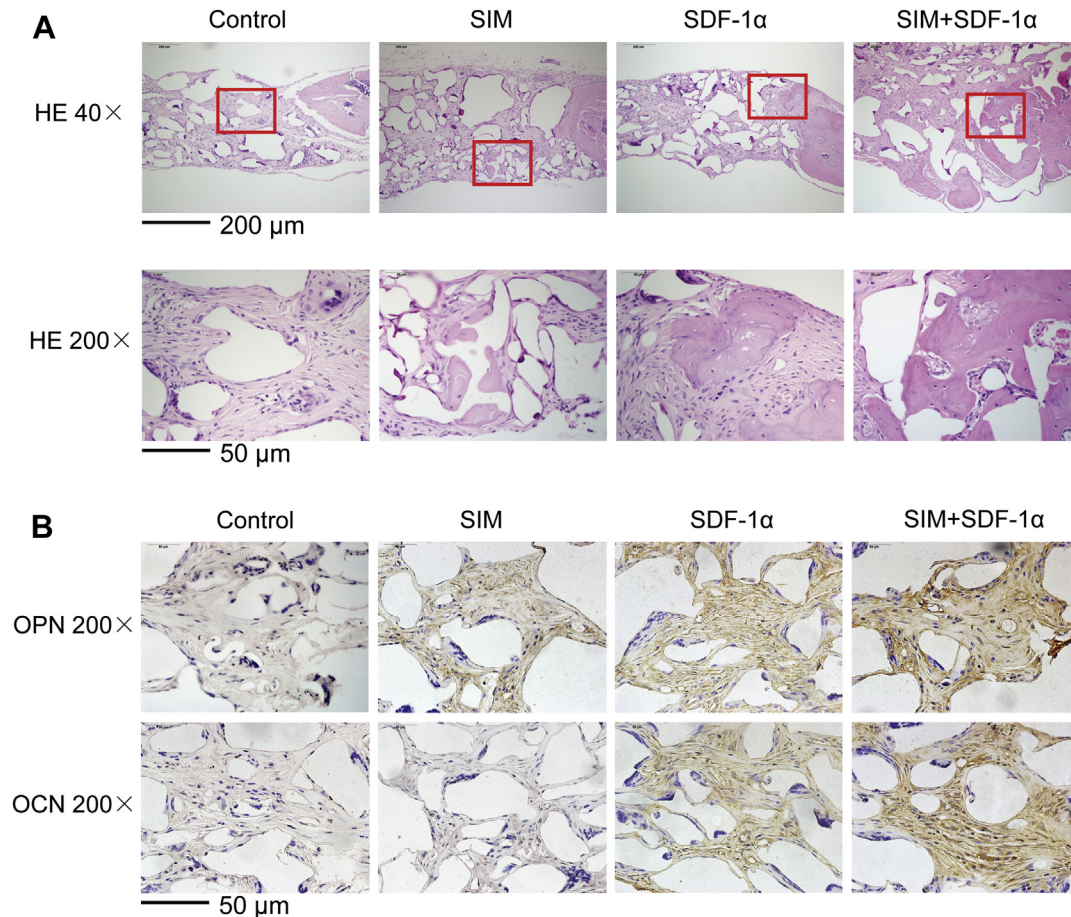
Fig. 4. Histological assessment of bone formation in each group. (A) HE staining. (B) Immunohistochemical staining for the osteogenic markers osteopontin (OPN) and osteocalcin (OCN).

composed of PLGA scaffold loaded with SDF-1α and SIM was constructed in this study. The application of this cell-free tissue engineering system means that isolation and ex vivo manipulation of cells can be avoided, and bone can be regenerated more efficiently and with less expense. To fully explore the bone regeneration capability and the underlying mechanisms of this new cell-homing approach, we carried out a series of systematic experiments in this study. Firstly, we investigated the optimal concentrations of SIM and SDF-1α for proliferation, osteogenesis and migration of mBMMSCs in vitro, and secondly, we demonstrated that bone formation in critical-sized calvarial defects in the mouse was significantly promoted by PLGA scaffold loaded with SDF-1α and SIM. Interestingly, we also found that SIM enhanced the chemotactic capability of SDF-1α in vitro and in vivo.

4.1. The effect of SDF-1α on the migration of mBMMSCs in vitro

It has been reported that the number of migrating MSCs increases in a dose-dependent manner at concentrations of 5–500 ng/ml [20,26]. In this study, we first investigated the in vitro chemotactic potency of SDF-1α and confirmed that SDF-1α promoted the migration of mBMMSCs in a dose-dependent manner. SDF-1α is the sole ligand for the chemokine receptor CXCR4 [52]. The interaction of SDF-1α with CXCR4 mediates homing of MSCs. Upon binding of SDF-1α to CXCR4, the receptor is stabilized into a conformation that activates the heterotrimeric G protein [53], which can regulate a wide variety of downstream pathways, including activation of phospholipase C and phosphoinositide-3

kinase, and inactivation of adenylyl cyclase. Signaling through the phosphoinositide-3 kinase pathway leads to the activation of p21-activated kinase (PAK) and cell polarization, the first step in migration. Phosphoinositide-3 kinase and various tyrosine kinases that activate Akt and Cdc42 are involved in actin polymerization. Phospholipase C-mediated events, such as calcium release and protein kinase C activation, as well as focal adhesion kinase, pyk2, paxillin and extracellular signal-regulated kinase are important in the adhesion process, leading to cell migration [54–58].

4.2. The effect of SIM on proliferation, osteogenesis and migration of mBMMSCs in vitro

To explore the effects of SIM on the proliferation and osteogenic differentiation of mBMMSCs in vitro, we performed cell proliferation and differentiation assays as we have previously reported [41], because cells with a different origin or from different species may react in different ways to SIM over a range of concentrations. In this study, we found that higher concentrations of SIM inhibited cell proliferation, but when the concentration was 0.2 μM or lower, it had a negligible effect on cell proliferation. We then tested ALP activity, a common marker used in osteogenic differentiation studies, and found that SIM increased ALP activity in mBMMSCs in a dose-dependent manner. Taking the results of cell proliferation and differentiation assays together, 0.2 μM SIM was determined to be the optimal acting concentration for mBMMSCs in this study.

The original intention of this study was to use SIM as an osteogenic factor in our cell-free bone tissue engineering system.
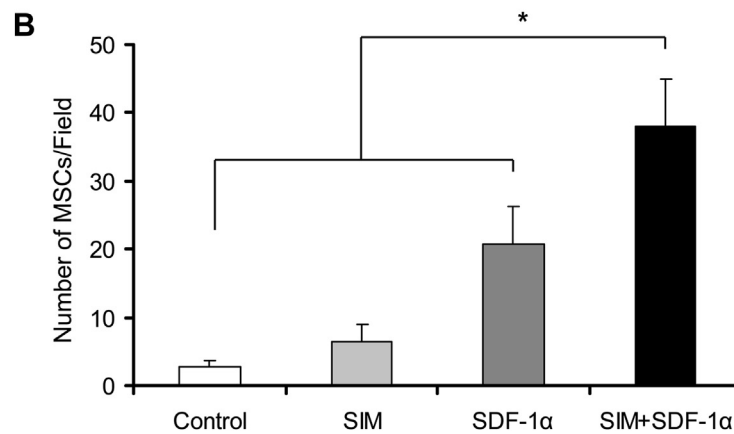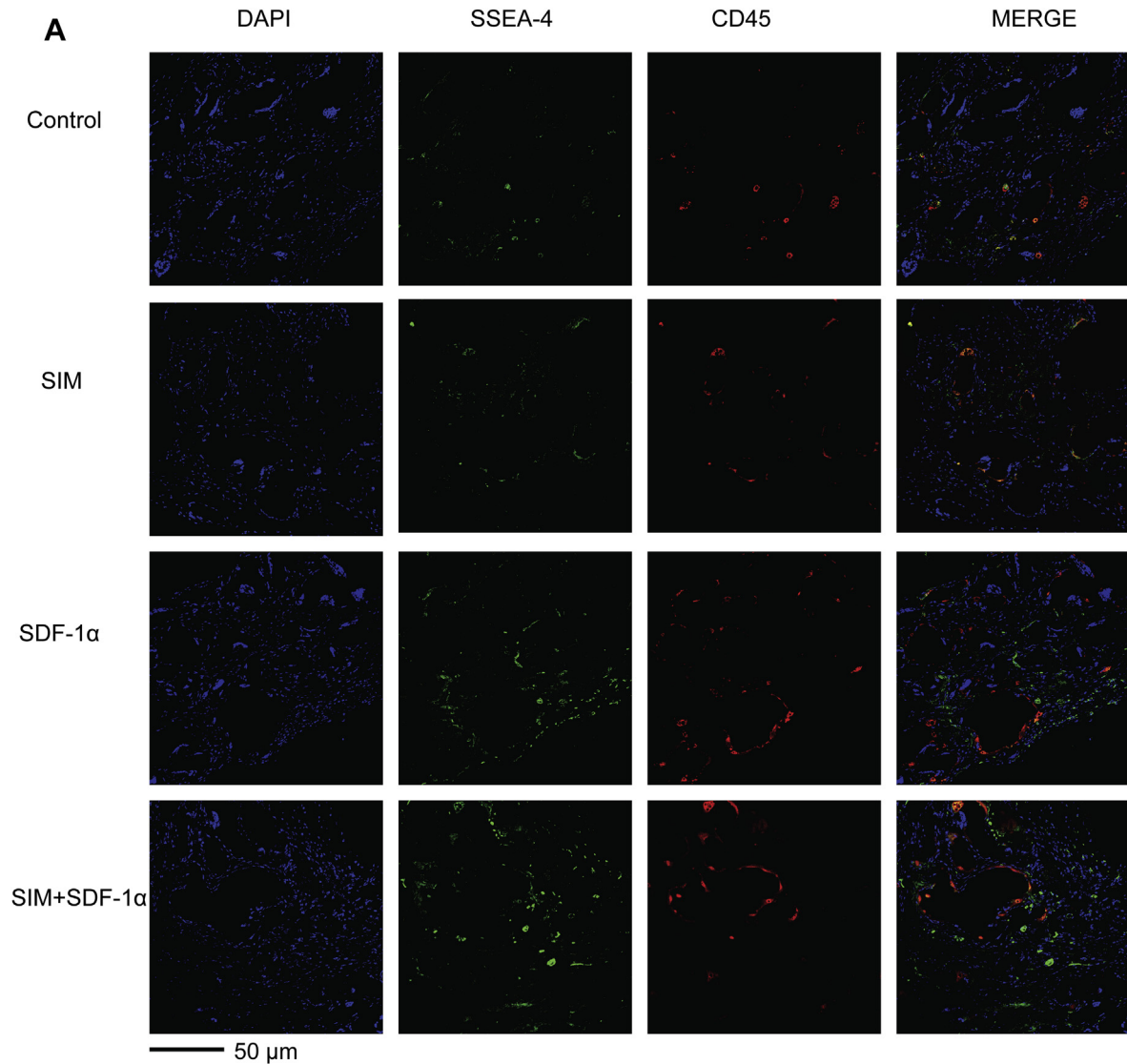
Fig. 5. Immunofluorescence staining showed that SDF-1α combined with SIM recruited more SSEA-4+/CD45− MSCs in vivo. (A) Immunofluorescence staining of the four groups. (B) Quantitative analysis of the numbers of recruited MSCs in the four groups. $*P < 0.05$.

Interestingly, however, we found that SIM at certain concentrations increased the migration of mBMMSCs. It has been well documented that SIM increases the osteogenic capability of MSCs [59]. However, the effects of SIM on the migration and homing of MSCs are a more recent finding. Cui et al. [46] reported that local application of SIM led to recruitment of autogenous osteogenic stem cells. Han et al. [47] reported that SIM mobilized the migration of BMMSCs to injured areas after spinal cord injury in rat. Our results were consistent with these studies. More importantly, when we combined SIM and SDF-1α, we found that the chemotactic capability of
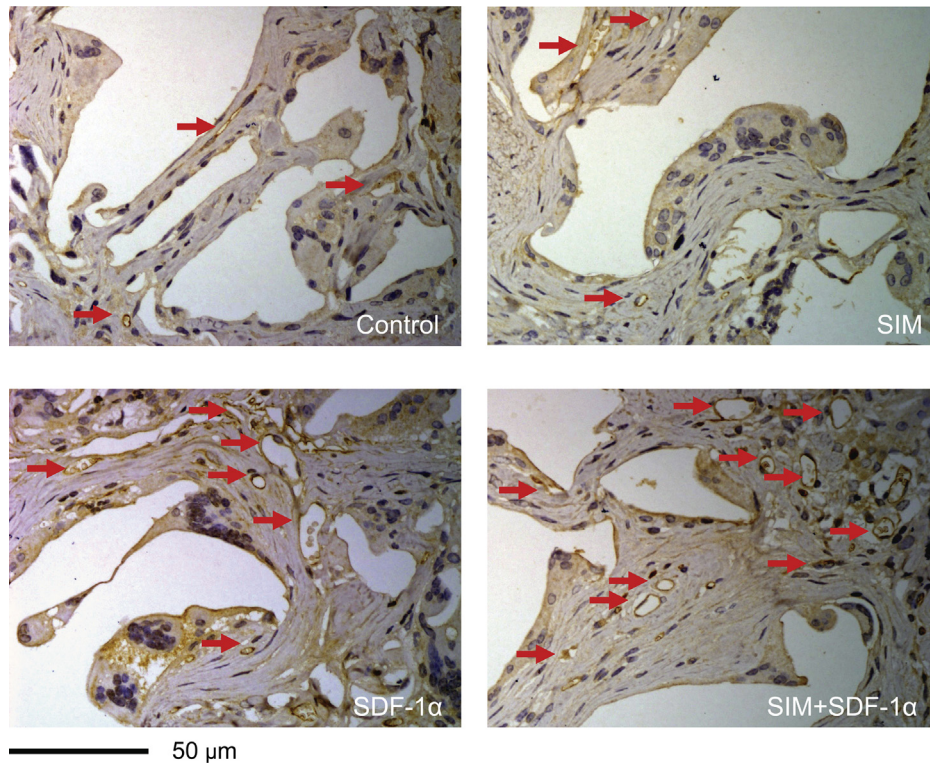
Fig. 6. IHC staining showed greater numbers of CD34-positive vascular endothelium cells (red arrows) in the SIM + SDF-1 group than in the other groups. (For interpretation of the references to color in this figure legend, the reader is referred to the web version of this article.)

SDF-1α was markedly enhanced. This cooperative effect between SIM and SDF-1α had new implications for the development of tissue-engineered bone systems. To confirm this cooperative effect and explore the underlying mechanisms we conducted further in vivo experiments.

4.3. Bone formation in a cell-free tissue-engineered bone system in mouse critical-sized calvarial defects, and preliminary exploration of the underlying mechanism

The cell-free tissue-engineered bone system in this study is composed simply of PLGA, SDF-1α and SIM. PLGA, as a copolymer of poly-lactic acid (PLA) and poly-glycolic acid (PGA), has been widely used in the medical field because it has good biodegradation properties and mechanical strength. Moreover, the clinical

application of PLGA has been approved by the FDA [60]. Another reason for choosing this scaffold in our study is because PLGA is a radiolucent material and once radiopaque areas develop, we know that there is mineralized tissue formation.

To investigate the in vivo bone formation capability of this cell-free tissue-engineered bone system, critical-sized [3,41] calvarial defects (4-mm diameter) were made in four groups of mice and filled with PLGA, PLGA + SIM, PLGA + SDF-1α or PLGA + SIM + SDF-1α. Six weeks after implantation, we observed that our cell-free tissue-engineered bone system (PLGA + SIM + SDF-1α) increased non-collagenous protein expression in the bone matrix and formed markedly more bone tissue than was seen in other groups.

To further explore the mechanism of bone formation in the cell-free tissue-engineered bone system, we studied MSC homing,
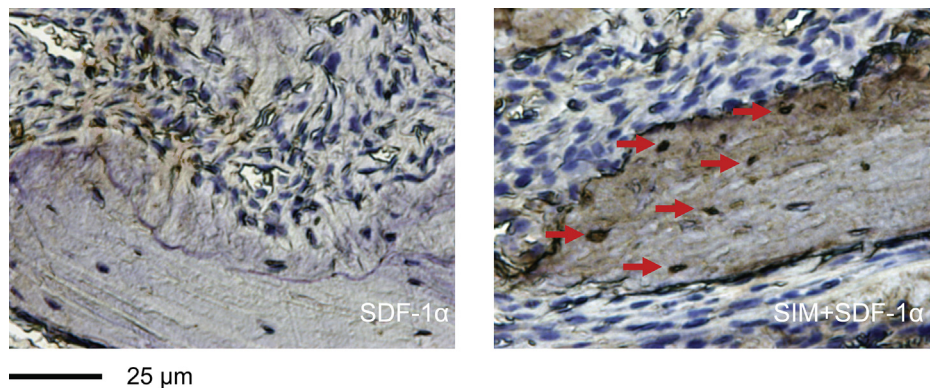
Fig. 7. IHC staining for BMP-2 in typical newly-formed bone tissue showed higher expression of BMP-2 in the SIM + SDF-1 group than the SIM group. No typical new bone structure was observed in either the control or SIM groups.

angiogenesis and BMP-2 expression in vivo. As reported by The-venot et al. [49], we detected SSEA4+/CD45− MSCs in the scaffold 1 week after implantation into the calvarial defect area. Because we used a cell-free system, the MSCs in the implantation site were assumed to come from circulating or surrounding MSC resources. Consistent with the in vitro experiments, we found that the SIM + SDF-1α group recruited more MSCs than other groups. These in vivo results confirmed that SIM increased the chemotactic capability of SDF-1α and enhanced MSC homing. It is well recognized that MSCs play essential roles in tissue regeneration and are they considered to be the basis of bone tissue engineering. Therefore, the cooperative effect of SIM and SDF-1α on MSC recruitment may be one explanation for the improved bone regeneration in critical-sized calvarial defects using the cell-free tissue-engineered bone system.

Mundy et al. discovered that statins (lovastatin and simvastatin) stimulate high expression of BMP-2 in osteoblasts, and can effectively stimulate bone formation [61]. We therefore tested the expression of BMP-2 in the newly-formed bone tissue and found that it was higher in the SIM + SDF-1α group than in the SDF-1α group. It has been reported that BMP-2 can directly induce osteoblastic differentiation by driving the expression of Runx2 and vice versa [62]. BMP-2 expression may therefore also play an important role in the improved bone regeneration seen in critical-sized calvarial defects using the cell-free tissue-engineered bone system.

Angiogenesis and vascularization are essential steps for the survival of engineered grafts after implantation [63]. We also studied the angiogenesis and vascularization capability of the cell-free tissue-engineered bone system by immunohistochemical staining of CD34+ vascular endothelium cells [50]. We found that improved vascularization was observed in the SIM + SDF-1α group compared to the other groups. It has been reported that SDF-1α can recruit endothelial progenitor cells and enhance vascularization in vivo [64]. Moreover, SIM can specifically increase the expression of BMP-2, which has also been shown to stimulate the expression of vascular endothelial growth factor (VEGF) and promote angiogenesis [65,66]. These cooperative effects on angiogenesis and vascularization may lead to improved bone regeneration.

There were some limitations to our study. Firstly, the application of SIM and SDF-1α in this study was simply by scaffold infusion and injection around the implantation site. In further studies, we plan to introduce a slow-release mechanism to improve the performance of our cell-free tissue-engineered bone system. Secondly, the exact mechanisms behind the cooperative effect of SIM and SDF-1α need to be further investigated on the basis of our current study.

5. Conclusions

SIM enhances the chemotactic capability of SDF-1α, and the cell-free bone tissue engineering system composed of SIM, SDF-1α and scaffold promotes bone regeneration in critical-sized calvarial defects in the mouse.

Acknowledgments

References

[1] Liu Y, Zhou Y, Feng H, Ma GE, Ni Y. Injectable tissue-engineered bone composed of human adipose-derived stromal cells and platelet-rich plasma. Biomaterials 2008;29:3338–45.

[2] Steinhardt Y, Aslan H, Regev E, Zilberman Y, Kallai I, Gazit D, et al. Maxillo-facial-derived stem cells regenerate critical mandibular bone defect. Tissue Eng Part A 2008;14:1763–73.

[3] Im JY, Min WK, You C, Kim HO, Jin HK, Bae JS. Bone regeneration of mouse critical-sized calvarial defects with human mesenchymal stem cells in scaffold. Lab Anim Res 2013;29:196–203.

[4] Zhou YS, Liu YS, Tan JG. Is 1, 25-dihydroxyvitamin D3 an ideal substitute for dexamethasone for inducing osteogenic differentiation of human adipose tissue-derived stromal cells in vitro? Chin Med J Engl 2006;119:1278–86.

[5] Liu Y, Zhao Y, Zhang X, Chen T, Zhao X, Ma GE, et al. Flow cytometric cell sorting and in vitro pre-osteoinduction are not requirements for in vivo bone formation by human adipose-derived stromal cells. PLoS One 2013;8:e56002.

[6] Castano-Izquierdo H, Alvarez-Barreto J, van den Dolder J, Jansen JA, Mikos AG, Sikavitsas VI. Pre-culture period of mesenchymal stem cells in osteogenic media influences their in vivo bone forming potential. J Biomed Mater Res A 2007;82:129–38.

[7] Stocum DL, Zupanc GK. Stretching the limits: stem cells in regeneration science. Dev Dyn 2008;237:3648–71.

[8] Bonab MM, Alimoghaddam K, Talebian F, Ghaffari SH, Ghavamzadeh A, Nikbin B. Aging of mesenchymal stem cell in vitro. BMC Cell Biol 2006;7:14.

[9] Crisostomo PR, Wang M, Wairiuko GM, Morrell ED, Terrell AM, Seshadri P, et al. High passage number of stem cells adversely affects stem cell activation and myocardial protection. Shock 2006;26:575–80.

[10] Kim K, Lee CH, Kim BK, Mao JJ. Anatomically shaped tooth and periodontal regeneration by cell homing. J Dent Res 2010;89:842–7.

[11] Yu L, Cecil J, Peng SB, Schrementi J, Kovacevic S, Paul D, et al. Identification and expression of novel isoforms of human stromal cell-derived factor 1. Gene 2006;374:174–9.

[12] Shirozu M, Nakano T, Inazawa J, Tashiro K, Tada H, Shinohara T, et al. Structure and chromosomal localization of the human stromal cell-derived factor 1 (SDF1) gene. Genomics 1995;28:495–500.

[13] Zlotnik A, Yoshie O. Chemokines: a new classification system and their role in immunity. Immunity 2000;12:121–7.

[14] Ma Q, Jones D, Borghesani PR, Segal RA, Nagasawa T, Kishimoto T, et al. Impaired B-lymphopoiesis, myelopoiesis, and derailed cerebellar neuron migration in CXCR4- and SDF-1-deficient mice. Proc Natl Acad Sci U S A 1998;95:9448–53.

[15] Nagasawa T, Hirota S, Tachibana K, Takakura N, Nishikawa S, Kitamura Y, et al. Defects of B-cell lymphopoiesis and bone-marrow myelopoiesis in mice lacking the CXC chemokine PBSF/SDF-1. Nature 1996;382:635–8.

[16] Zou YR, Kottmann AH, Kuroda M, Taniuchi I, Littman DR. Function of the chemokine receptor CXCR4 in haematopoiesis and in cerebellar development. Nature 1998;393:595–9.

[17] Aiuti A, Tavian M, Cipponi A, Ficara F, Zappone E, Hoxie J, et al. Expression of CXCR4, the receptor for stromal cell-derived factor-1 on fetal and adult human lympho-hematopoietic progenitors. Eur J Immunol 1999;29:1823–31.

[18] Baggiolini M. Chemokines and leukocyte traffic. Nature 1998;392:565–8.

[19] Yu X, Huang Y, Collin-Osdoby P, Osdoby P. Stromal cell-derived factor-1 (SDF-1) recruits osteoclast precursors by inducing chemotaxis, matrix metalloproteinase-9 (MMP-9) activity, and collagen transmigration. J Bone Miner Res 2003;18:1404–18.

[20] Ji JF, He BP, Dheen ST, Tay SS. Interactions of chemokines and chemokine receptors mediate the migration of mesenchymal stem cells to the impaired site in the brain after hypoglossal nerve injury. Stem Cells 2004;22:415–27.

[21] Zhao T, Zhang D, Millard RW, Ashraf M, Wang Y. Stem cell homing and angiomyogenesis in transplanted hearts are enhanced by combined intra-myocardial SDF-1alpha delivery and endogenous cytokine signaling. Am J Physiol Heart Circ Physiol 2009;296:H976–86.

[22] Ratajczak MZ, Majka M, Kucia M, Drukala J, Pietrzkowski Z, Peiper S, et al. Expression of functional CXCR4 by muscle satellite cells and secretion of SDF-1 by muscle-derived fibroblasts is associated with the presence of both muscle progenitors in bone marrow and hematopoietic stem/progenitor cells in muscles. Stem Cells 2003;21:363–71.

[23] Hatch HM, Zheng D, Jorgensen ML, Petersen BE. SDF-1alpha/CXCR4: a mechanism for hepatic oval cell activation and bone marrow stem cell recruitment to the injured liver of rats. Cloning Stem Cells 2002;4:339–51.

[24] Togel F, Isaac J, Hu Z, Weiss K, Westenfelder C. Renal SDF-1 signals mobilization and homing of CXCR4-positive cells to the kidney after ischemic injury. Kidney Int 2005;67:1772–84.

[25] Ceradini DJ, Kulkarni AR, Callaghan MJ, Tepper OM, Bastidas N, Kleinman ME, et al. Progenitor cell trafficking is regulated by hypoxic gradients through HIF-1 induction of SDF-1. Nat Med 2004;10:858–64.

[26] Kitaori T, Ito H, Schwarz EM, Tsutsumi R, Yoshitomi H, Oishi S, et al. Stromal cell-derived factor 1/CXCR4 signaling is critical for the recruitment of mesenchymal stem cells to the fracture site during skeletal repair in a mouse model. Arthritis Rheum 2009;60:813–23.

[27] Otsuru S, Tamai K, Yamazaki T, Yoshikawa H, Kaneda Y. Circulating bone marrow-derived osteoblast progenitor cells are recruited to the bone-forming site by the CXCR4/stromal cell-derived factor-1 pathway. Stem Cells 2008;26: 223–34.

[28] Hosogane N, Huang Z, Rawlins BA, Liu X, Boachie-Adjei O, Boskey AL, et al. Stromal derived factor-1 regulates bone morphogenetic protein 2-induced osteogenic differentiation of primary mesenchymal stem cells. Int J Biochem Cell Biol 2010;42:1132—41.

[29] Cei S, Kandler B, Fugl A, Gabriele M, Hollinger JO, Watzek G, et al. Bone marrow stromal cells of young and adult rats respond similarly to platelet-released supernatant and bone morphogenetic protein-6 in vitro. J Periodontol 2006;77:699—706.

[30] Fujii M, Takeda K, Imamura T, Aoki H, Sampath TK, Enomoto S, et al. Roles of bone morphogenetic protein type I receptors and Smad proteins in osteoblast and chondroblast differentiation. Mol Biol Cell 1999;10:3801—13.

[31] Gu K, Zhang L, Jin T, Rutherford RB. Identification of potential modifiers of Runx2/Cbfa1 activity in C2C12 cells in response to bone morphogenetic protein-7. Cells Tissues Organs 2004;176:28—40.

[32] Katagiri T, Yamaguchi A, Komaki M, Abe E, Takahashi N, Ikeda T, et al. Bone morphogenetic protein-2 converts the differentiation pathway of C2C12 myoblasts into the osteoblast lineage. J Cell Biol 1994;127:1755—66.

[33] Yeh LC, Tsai AD, Lee JC. Osteogenic protein-1 (OP-1, BMP-7) induces osteoblastic cell differentiation of the pluripotent mesenchymal cell line C2C12. J Cell Biochem 2002;87:292—304.

[34] Zachos TA, Shields KM, Bertone AL. Gene-mediated osteogenic differentiation of stem cells by bone morphogenetic proteins-2 or -6. J Orthop Res 2006;24: 1279—91.

[35] Zhu W, Kim J, Cheng C, Rawlins BA, Boachie-Adjei O, Crystal RG, et al. Noggin regulation of bone morphogenetic protein (BMP) 2/7 heterodimer activity in vitro. Bone 2006;39:61—71.

[36] Chen D, Zhao M, Mundy GR. Bone morphogenetic proteins. Growth Factors 2004;22:233—41.

[37] Zhang X, Guo J, Zhou Y, Wu G. The roles of bone morphogenetic proteins and their signaling in the osteogenesis of adipose-derived stem cells. Tissue Eng Part B Rev; 2013. http://dx.doi.org/10.1089/ten.teb.2013.0204 [Ahead of print].

[38] Wang CK, Ho ML, Wang GJ, Chang JK, Chen CH, Fu YC, et al. Controlled-release of rhBMP-2 carriers in the regeneration of osteonecrotic bone. Biomaterials 2009;30:4178—86.

[39] Benglis D, Wang MY, Levi AD. A comprehensive review of the safety profile of bone morphogenetic protein in spine surgery. Neurosurgery 2008;62: ONS423—31.

[40] Chen NF, Smith ZA, Stiner E, Armin S, Sheikh H, Khoo LT. Symptomatic ectopic bone formation after off-label use of recombinant human bone morphogenetic protein-2 in transforaminal lumbar interbody fusion. J Neurosurg Spine 2010;12:40—6.

[41] Zhou Y, Ni Y, Liu Y, Zeng B, Xu Y, Ge W. The role of simvastatin in the osteogenesis of injectable tissue-engineered bone based on human adipose-derived stromal cells and platelet-rich plasma. Biomaterials 2010;31:5325—31.

[42] Stein D, Lee Y, Schmid MJ, Killpack B, Genrich MA, Narayana N, et al. Local simvastatin effects on mandibular bone growth and inflammation. J Periodontol 2005;76:1861—70.

[43] Nyan M, Sato D, Oda M, Machida T, Kobayashi H, Nakamura T, et al. Bone formation with the combination of simvastatin and calcium sulfate in critical-sized rat calvarial defect. J Pharmacol Sci 2007;104:384—6.

[44] Wu Z, Liu C, Zang G, Sun H. The effect of simvastatin on remodelling of the alveolar bone following tooth extraction. Int J Oral Maxillofac Surg 2008;37:170—6.

[45] Ozec I, Kilic E, Gumus C, Goze F. Effect of local simvastatin application on mandibular defects. J Craniofac Surg 2007;18:546—50.

[46] Cui Y, Han X, Wang J, Song Q, Tan J, Fu X, et al. Calvarial defect healing by recruitment of autogenous osteogenic stem cells using locally applied simvastatin. Biomaterials 2013;34:9373—80.

[47] Han X, Yang N, Cui Y, Xu Y, Dang G, Song C. Simvastatin mobilizes bone marrow stromal cells migrating to injured areas and promotes functional recovery after spinal cord injury in the rat. Neurosci Lett 2012;521:136—41.

[48] Nadri S, Soleimani M, Hosseni RH, Massumi M, Atashi A, Izadpanah R. An efficient method for isolation of murine bone marrow mesenchymal stem cells. Int J Dev Biol 2007;51:723—9.

[49] Thevenot PT, Nair AM, Shen J, Lotfi P, Ko C-Y, Tang L. The effect of incorporation of SDF-1α into PLGA scaffolds on stem cell recruitment and the inflammatory response. Biomaterials 2010;31:3997—4008.

[50] Asahara T, Murohara T, Sullivan A, Silver M, van der Zee R, Li T, et al. Isolation of putative progenitor endothelial cells for angiogenesis. Science 1997;275: 964—7.

[51] Gang EJ, Bosnakovski D, Figueiredo CA, Visser JW, Perlingeiro RC. SSEA-4 identifies mesenchymal stem cells from bone marrow. Blood 2007;109:1743—51.

[52] Chemokine/chemokine receptor nomenclature. Cytokine 2003;21:48—9.

[53] Holland JD, Kochetkova M, Akekawatchai C, Dottore M, Lopez A, McColl SR. Differential functional activation of chemokine receptor CXCR4 is mediated by G proteins in breast cancer cells. Cancer Res 2006;66:4117—24.

[54] Wong D, Korz W. Translating an antagonist of chemokine receptor CXCR4: from bench to bedside. Clin Cancer Res 2008;14:7975—80.

[55] Ganju RK, Brubaker SA, Meyer J, Dutt P, Yang Y, Qin S, et al. The alpha-chemokine, stromal cell-derived factor-1alpha, binds to the transmembrane G-protein-coupled CXCR-4 receptor and activates multiple signal transduction pathways. J Biol Chem 1998;273:23169—75.

[56] Zhao M, Discipio RG, Wimmer AG, Schraufstatter IU. Regulation of CXCR4-mediated nuclear translocation of extracellular signal-related kinases 1 and 2. Mol Pharmacol 2006;69:66—75.

[57] Busillo JM, Benovic JL. Regulation of CXCR4 signaling. Biochim Biophys Acta 2007;1768:952—63.

[58] Chinni SR, Sivalogan S, Dong Z, Filho JC, Deng X, Bonfil RD, et al. CXCL12/CXCR4 signaling activates Akt-1 and MMP-9 expression in prostate cancer cells: the role of bone microenvironment-associated CXCL12. Prostate 2006;66:32—48.

[59] Qi Y, Zhao T, Yan W, Xu K, Shi Z, Wang J. Mesenchymal stem cell sheet transplantation combined with locally released simvastatin enhances bone formation in a rat tibia osteotomy model. Cytotherapy 2013;15:44—56.

[60] Jain RA. The manufacturing techniques of various drug loaded biodegradable poly(lactide-co-glycolide) (PLGA) devices. Biomaterials 2000;21:2475—90.

[61] Mundy G, Garrett R, Harris S, Chan J, Chen D, Rossini G, et al. Stimulation of bone formation in vitro and in rodents by statins. Science 1999;286:1946—9.

[62] Choi KY, Kim HJ, Lee MH, Kwon TG, Nah HD, Furuichi T, et al. Runx2 regulates FGF2-induced Bmp2 expression during cranial bone development. Dev Dyn 2005;233:115—21.

[63] Kanczler JM, Oreffo RO. Osteogenesis and angiogenesis: the potential for engineering bone. Eur Cell Mater 2008;15:100—14.

[64] Stellos K, Langer H, Daub K, Schoenberger T, Gauss A, Geisler T, et al. Platelet-derived stromal cell-derived factor-1 regulates adhesion and promotes differentiation of human CD34+ cells to endothelial progenitor cells. Circulation 2008;117:206—15.

[65] Bouletreau PJ, Warren SM, Spector JA, Peled ZM, Gerrets RP, Greenwald JA, et al. Hypoxia and VEGF up-regulate BMP-2 mRNA and protein expression in microvascular endothelial cells: implications for fracture healing. Plast Reconstr Surg 2002;109:2384—97.

[66] Deckers MM, van Bezooijen RL, van der Horst G, Hoogendam J, van Der Bent C, Papapoulos SE, et al. Bone morphogenetic proteins stimulate angiogenesis through osteoblast-derived vascular endothelial growth factor A. Endocrinology 2002;143:1545—53.